Adapting a cMUT transducer to detect acoustic emissions

D. Ozevin and S.P. Pessiki
Department of Civil and Environmental Engineering
Lehigh University, Bethlehem, PA, USA

D.W. Greve and I.J. Oppenheim
Department of Civil and Environmental Engineering,
Carnegie Mellon University, Pittsburgh, PA, USA

***Abstract*—Acoustic emissions are ultrasonic pulses produced in solids when irreversible damage, such as material yielding or crack extension, occurs under mechanical loading. We report on the design, fabrication, and experimental demonstration of a cMUT transducer specifically designed for measurement of acoustic emission events by detecting ultrasonic waves in the 100 kHz to 1 MHz range. The cMUT transducer is intended to replace the commonly used underdamped resonant PZT transducer. In this novel application the ultrasonic energy is coupled to the substrate and the motion of the substrate relative to the supended diaphragm provides an electrical signal. This application requires a very different device design, underdamped and lower in resonant frequency than a cMUT intended for high frequency imaging. We report here the engineering of the quality factor by appropriate spacing of the etch release holes and the fabrication of transducers with multiple resonant frequencies on the same chip. We will also report the detection of actual acoustic emission events and we will compare the cMUT transducers with conventional PZT transducers.**

Keywords-component; capacitive, MEMS, acoustic emission

I. INTRODUCTION

Detection of acoustic emission events in structures under stress is often used to assess the health of the stucture. Acoustic emission occurs as a result of crack growth and other failure mechanisms and results in the emission of bursts of ultrasonic energy with most of the energy between about 100 kHz and 1 MHz [1]. The most commonly used transducers are piezoelectric transducers that are either resonant or broadband. Generally speaking resonant transducers have moderate Q values which make it possible to distinguish between bursts that are closely spaced in time. In contrast, broadband transducers respond to emissions over the entire range of frequencies but generally have lower sensitivity.

This work is directed at the development and demonstration of MEMS-based transducers for acoustic emission. A MEMS transducer was reported by Jones et al. [2] and its response to pencil-break excitation was studied. To the best of our knowledge the detection of failure-induced acoustic emission signals by a MEMS transducer has not yet been reported. MEMS-based transducers could eventually be integrated with data-processing electronics and could be low in cost. More immediately, MEMS makes it possible to fabricate several resonant transducers on the same chip. Multiple transducers could be used to detect acoustic emission energy at several different frequencies. This additional information should provide improved understanding of the damage processes and in addition should help discriminate between mechanical noise and true acoustic emission events.

We have chosen to adapt the capacitive MEMS ultrasonic transducer (cMUT) [3] for this application. In contrast to the usual applications for this device, in this case the ultrasonic energy is coupled to the substrate and causes the suspended diaphragm to move with respect to the substrate. It is necessary to engineer the dimensions of the diaphragm in order to obtain resonant frequencies in range of interest (100 kHz to 1 MHz) and also to obtain appropriate Q values.

II. TRANSDUCER DESIGN

Figure 1 compares a conventional piezoelectric acoustic emission transducer [4] with a MEMS transducer. In the case of the piezoelectric transducer, ultrasonic vibrations of the transmitting medium are coupled to a PZT element causing a terminal voltage $v(t)$ proportional to the strain. The backing material is chosen to provide the appropriate amount of damping for the desired transducer bandwidth. In contrast, in the case of the MEMS transducer the ultrasonic vibrations are coupled to the bottom plate of a capacitive transducer. Vibrations of the bottom plate with respect to the top plate cause a current $i(t) = V_{DC}(dC/dt)$ in the external circuit where V_{DC} is the DC bias voltage and C is the capacitance. In this case the peak frequency $\omega_0 = \sqrt{k/m}$ where k is the effective spring constant and m is the effective mass of the top plate. The bandwidth is determined by squeeze-film damping [5] due to the presence of etch release holes in the top diaphragm.

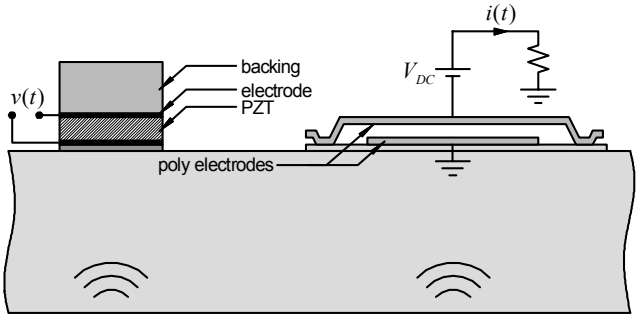

Figure 1. Conventional piezoelectric (left) and MEMS (right) transducers for acoustic emission. (Schematic only, the two detector types are not drawn to the same scale).

The cMUT devices used in this work were fabricated in the multi-user MUMPS process. This process has three polysilicon structural layers; in this work the diaphragms are formed between the POLY0 and POLY1 layers. The top diaphragm is 2.0 µm in thickness and the gap between the two polysilicon layers was 1.25 µm. The chip was 1 cm^2 in size and contained seven transducers with different resonant frequencies.

Usually cMUT devices have diaphragms supported on all edges; in this case the effective spring constant k is high, leading to resonant frequencies in the MHz region [3,5]. In order to obtain lower resonant frequencies we have used a design in which a sheet of polysilicon is supported by a small number of cross-shaped springs (Figure 2). In order to obtain underdamped behavior at these lower frequencies it is necessary to provide the appropriate number of etch holes (also visible in Figure 2).

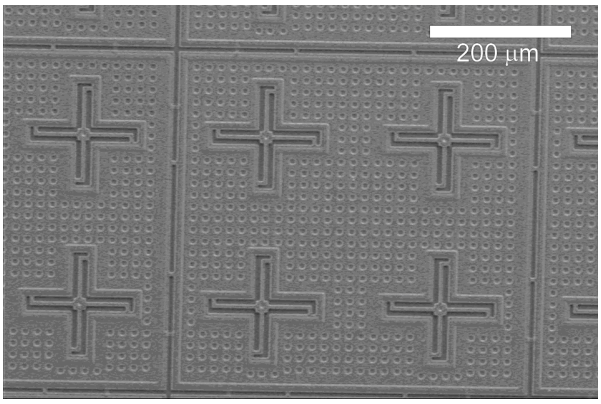

Figure 2. Scanning electron micrograph showing top diaphragm of a piston-type transducer. The cross-shaped springs and the etch release holes are visible.

The chip consists of transducers with seven different resonant frequencies ranging from about 100 kHz to 1 MHz along with some additional test structures (Figure 3). For testing the completed chips are attached to a 64-pin ceramic package with silver epoxy and pads are wire-bonded to the pins.

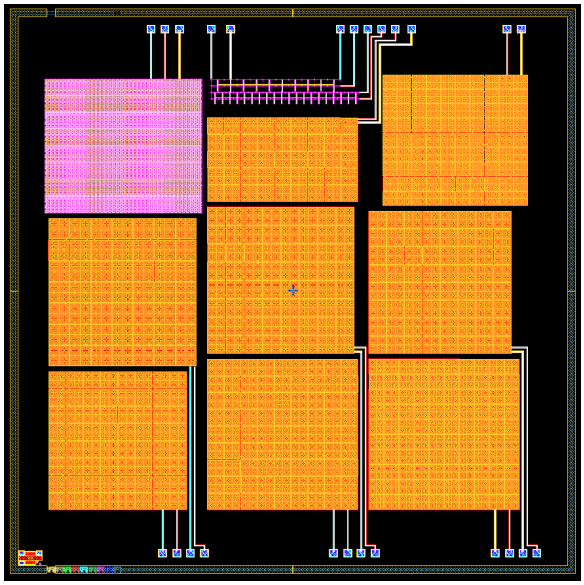

Figure 3. CAD layout of the chip.

Table I summarizes the characteristics of the seven different transducers. In this table, n is the number of individual elements connected in parallel; L_{s1} and L_{s2} are the length of the short and long spring segments, respectively; L_m is the size of each element, and A is the total area of the transducer. The resonant frequencies measured in vacuum are f_{p1} and f_{p2}.

Table I. Characteristics of MEMS transducers.

	C1	C2	C3	D1	D2	D3	B3
n	49	64	64	64	81	100	90
L_{s1} [µm]	8	8	8	8	8	8	8
L_{s2} [µm]	45	40	33	27	22	19	12
L_m [µm]	380	330	320	310	300	270	240
A [mm^{-2}]	7.23	7.16	6.73	6.32	7.51	7.53	6.29
f_{p1} [kHz]	107	150	178	187	210	272	-
f_{p2} [kHz]	150	207	252	275	317	405	925

The resonant frequency and damping of transducers can be determined from admittance measurements with an applied DC bias. Figure 4 shows admittance measurements on transducer D2. The transducer exhibits two closely spaced resonant modes which correspond to a vertical motion of the entire diaphragm (lower resonance) and a mode with a rocking motion (upper resonance) [6]. Extracted values of the Q for the lowest mode of the D2 transducer is 2.5. Similar values are obtained with other transducers, corresponding to the desired underdamped condition for resonant transducers.

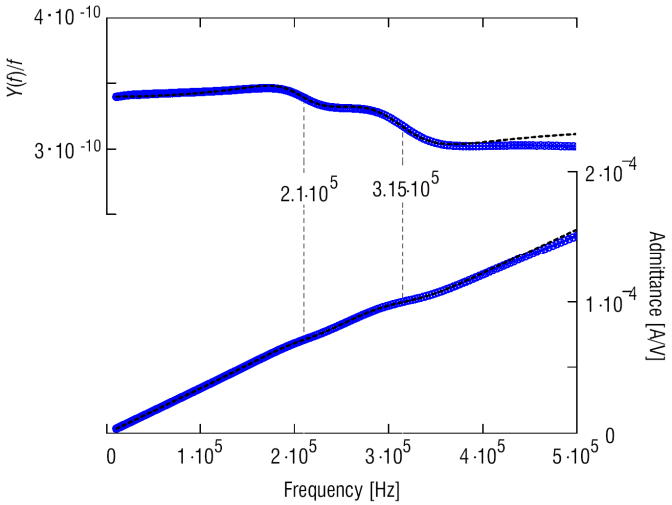

Figure 4. Measured admittance magnitude as a function of frequency for D2 transducer with a DC bias of 10 V. Also shown is a fit to the impedance magnitude using two modes.

III. TRANSDUCER TESTING

The MEMS transducers were tested and compared with a conventional piezoelectric transducer (Physical Acoustics Corporation R30). Figure 5 shows the test setup. The cMUT chip and the conventional acoustic emission transducer were attached to a pre-cracked rectangular steel beam specimen 76 cm

in length that was loaded in 4-point bending in a testing machine. Signals from five different cMUT transducers were collected along with the signal from the conventional transducer. The cMUT transducers were biased with a DC voltage of 9 V. The signals were amplified and digitized by either a National Instruments 5122 DAQ board or a Tektronix TDS2014 oscilloscope. Labview programs were used to control the testing machine and data acquisition. Trigger signals for the oscilloscope and DAQ board were obtained from the conventional piezoelectric transducer. After each trigger event records were written to hard disk under computer control. The testing machine load and displacement were also recorded as a function of time for correlation with the acoustic emission records.

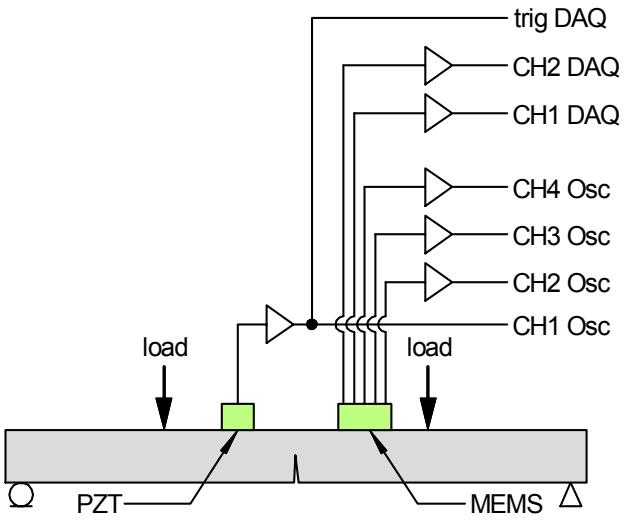

Figure 5. Experimental arrangement for transducer testing.

We report results here for one complete experiment in which a test specimen was loaded into the failure range. The crosshead displacement was increased linearly at a rate of 0.025 mm/min. Figure 6 shows the measured displacement of the crosshead as a function of the load. Acoustic emission events detected by the piezoelectric transducer are indicated as red circles. Initially the displacement is a linear function of the load (Hooke's law) and in this region no acoustic emission events are observed. At about 20 kN acoustic emission events begin to be observed and the load-displacement plot becomes distinctly nonlinear. A large load drop occurs at about 23.5 kN; this is associated with a substantial amount of crack propagation. After this load drop acoustic emission events continue to be observed until a second load drop, at which point the experiment was terminated.

Note that in Figure 6 an appreciable number of acoustic emission events are observed prior to the first load drop. Detection of these events is the objective of acoustic emission testing, as these events indicate that the member is sustaining damage and crack growth. In the following, we will compare the acoustic emission events detected by the conventional piezoelectric and MEMS transducers.

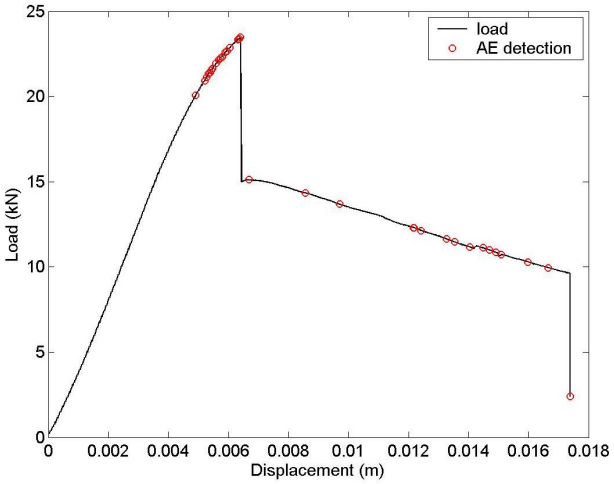

Figure 6. Load-displacement characteristic with acoustic emission events detected by the conventional transducer indicated as red circles.

Figure 7 compares the signal from the C2 MEMS transducer and the piezoelectric transducer for an acoustic emission event at a load of 21.3 kN. Both transducers unambiguously detect the acoustic emission event although the piezoelectric transducer has a larger signal level and better signal to noise ratio. The lower signal level of the MEMS transducer is a consequence of the generally superior value for the transformer ratio n for piezoelectric transducers. (The transformer ratio $n = -i/u$ is the ratio between the output electrical current i and the wave velocity u). The higher noise level is in part due to electrical interference in the arrangement used for this work.

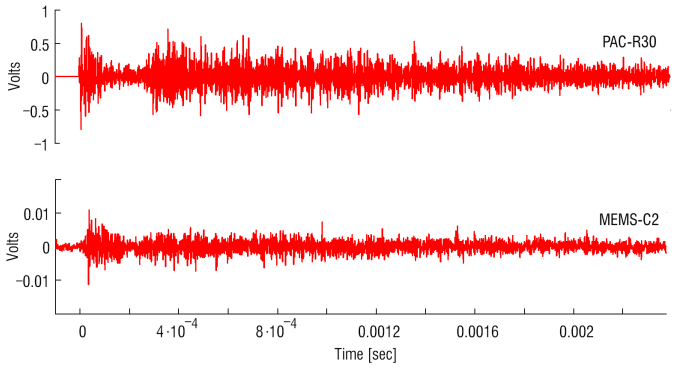

Figure 7. Comparison of signals detected by the piezoelectric transducer (top trace) and the MEMS transducer (bottom trace) at 21.3 kN.

Because of the lower signal-to-noise ratio, not all acoustic emission events detected with the piezoelectric transducer were detected by the MEMS transducer. Figure 8 compares the signal levels and the detected events for the two types of transducers. A total of 33 events were detected by the piezoelectric transducer. The left-hand plot records the maximum signal level during the event; signals ranged from tenths of a volt to above one volt (the saturation limit of the oscilloscope). The right-hand plot shows the maximum signal level recorded by the C2 MEMS transducer during the 33 detected acoustic emission events. Some events did not give a clear signal above the noise for the MEMS transducer (open points). A significant

fraction of the events were successfully detected, however, including a number of events which occurred prior to the load drop at 23.5 kN. This experiment shows that the present MEMS transducer design is sufficiently sensitive to detect acoustic events indicative of damage and crack growth.

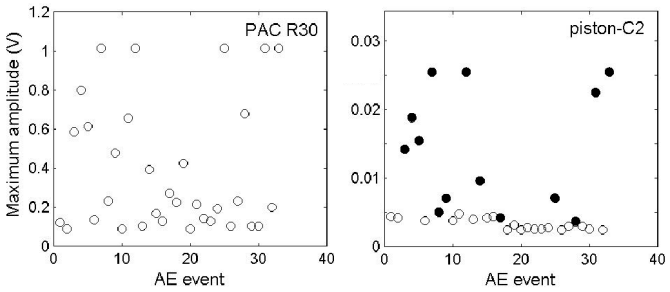

Figure 8. Comparison of MEMS and piezoelectric transducers for 33 events: (left) peak signal levels detected by the piezoelectric transducer and (right) peak signal levels detected by the C2 MEMS transducer in the same time intervals. Filled points indicate acoustic emission events that were clearly seen above the noise level.

MEMS transducers offer the possibility of simultaneous detection by multiple redundant transducers and/ or detection by transducers with different resonant frequencies. This may make it possible to discriminate between real and spurious signals. Simultaneous detection by five different transducers is shown in Figure 8 at a load of 21.1 kN (prior to the first load drop). This event is clearly detected by all five transducers.

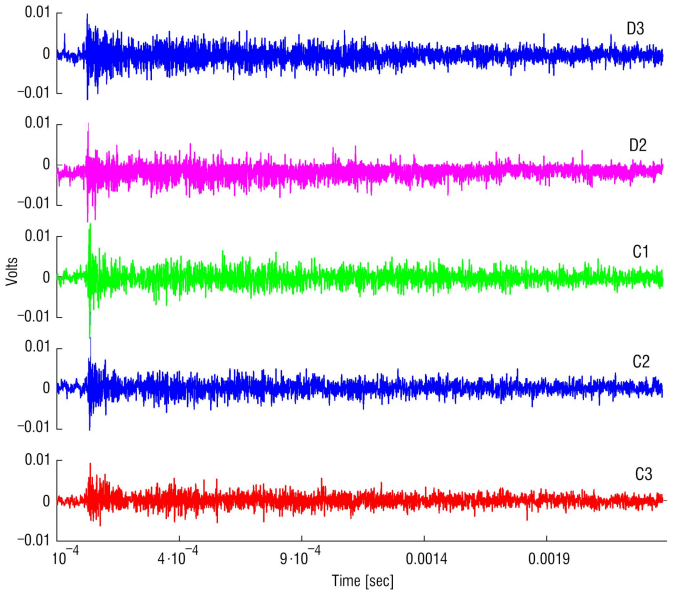

Figure 9. Signals detected by five different MEMS transducers at 21.1 kN.

IV. Summary

We have shown that the cMUT can be adapted to be a practical transducer for acoustic emission signals. The resonant frequency of the transducer is determined by the spring constant and the effective mass of the supported diaphragm. In contrast to cMUT intended for ultrasonic imaging, moderate underdamping is desired. This has been achieved by appropriate choice of the spacing of etch release holes.

In this work we have demonstrated the detection of acoustic emission events that signal the imminent failure of a structural member. However, not all the acoustic emission events detected by a conventional piezoelectric transducer were detected by the MEMS transducer. This is a consequence of the somewhat worse signal-to-noise ratio of the MEMS transducer, in part as a result of electrical interference. We believe that the signal-to-noise ratio can be improved with better packaging and shielding.

Acknowledgment

The authors would like to thank N. Tyson for the admittance measurements. We also thank the Pennsylvania Infrastructure Technology Alliance and the National Science Foundation for support. This material is based upon work supported by the National Science Foundation under Grant No. CMS-0329880. Any opinions, findings, and conclusions or recommendations expressed in this material are those of the authors and do not necessarily reflect the views of the National Science Foundation.

References

[1] Stephens, R.W., and Pollock, A.A., "Waveforms and Frequency Spectra of Acoustic Emission," Journal of the Acoustical Society of America, Vol. 50, No. 3, 1971, pp. 904-910.

[2] A.R.D. Jones, R.A. Noble, R.J. Bozeat, and D.A. Hutchins, "Micromachined Ultrasonic Transducers for Damage Detection in CFRP Composites," *Proceedings of the SPIE*, vol. 3673, 1999, pp. 369-78.

[3] X. Jin, O. Oralkan, F.L. Degertekin, and B.T. Khuri-Yakub, "Characterization of one-dimensional capacitive micromachined ultrasonic immersion transducer arrays," *IEEE Transactions on Ultrasonics, Ferroelectrics, and Frequency Control*, vol. 48, pp. 750-760 (2001).

[4] Gautschi, G., Piezoelectric Sensorics, Springer-Verlag, 2001, 1st Edition.

[5] Oppenheim, I.J., Jain, A., and Greve, D.W., "Electrical Characterization of Coupled and Uncoupled MEMS Ultrasonic Transducers," IEEE Transactions on Ultrasonics, Ferroelectrics, and Frequency Control, Vol. 50, No. 3, March 2003, pp. 297-304.

[6] Ozevin, D., Greve. D. W., Oppenheim, I. J., and Pessiki, S. P., "Steel Plate Coupled Behavior of MEMS Transducer Developed for Acoustic Emission Testing," *26th European Conference on Acoustic Emission Testing*, Berlin, September 2004.